6-Triethylenetetramine 6-deoxycellulose grafted with crotonaldehyde as adsorbent for Cr^{6+} removal from wastewater

Ahmed Eleryan[1], Ahmed El Nemr[1*], Mohammad Mashaly[2], Azza Khaled[1]

Abstract— Rice husk cellulose was isolated and tosylated with p-toluenesulphonyl chloride followed by substitution with triethylenetetramine to give 6-Triethylenetetramine 6-deoxycellulose. This was then grafted with crotonaldehyde in the presence of $FeCl_3$ and the product was evaluated as a biosorbent for the removal of Cr^{6+} ions from wastewater. The unloaded and loaded biosorbent with Cr^{6+} ions were characterized by FTIR, SEM and EDX analysis. The maximum adsorption of Cr^{6+} ions was achieved at acidic pH (1.5). The adsorption data was fitted better with Langmuir isotherm than Freundlich model indicating that the adsorption mechanism is mono layer adsorption. The maximum adsorption capacity of Cr^{6+} ions obtained from Langmuir isotherm model was 196.08 mg/g. The adsorption process followed the pseudo second order kinetic with a rate constant ranged from 0.0003 to 0.3 g/mg/h.

Index Terms— Cellulose, *p*-toluenesulphonyl chloride, Triethylenetetramine, crotonaldehyde, adsorption, chromium, removal.

1 Introduction

Chemically modified cellulose has great benefits and used in many applications in different fields such as pollutants removing from aquatic environment or industrial wastewater treatment [1,2]. Modification of cellulose as a carbohydrate polymer achieved via the reaction of the free hydroxyl groups present on the unhydroglucose unit of the cellulose chain polymer [3,4]. Hydroxyl groups undergo many reactions as estrification, etherification, nitration, sulfonation … etc according to the target functional group suitable for application. Cellulose can be grafted or cross-linked with organic moieties to enhance its adsorption efficiency [5,6]. The use of functionalized cellulose in removal of various pollutants has been adequately reviewed and chelating ability of modified cellulose can be improved by specific functionalization [4]. It is reported that, the presence of nitrogen containing groups like tetra-amines linked to cellulose have been found to enhance the bio-sorbent capacity of cellulose [7].

Several thousand cubic meters of toxic effluents containing hazardous chemicals and metal ions complexes are ejected every day into the aquatic environment from various industrial processes and urbanization [8]. Great efforts must be done to remove these pollutants and treat these effluents especially that contain heavy metal ions to decrease their concentrations to the safe limits. One of the most toxic heavy metal ions is chromium which exists in two stable oxidation, trivalent (Cr^{3+}) and hexavalent (Cr^{6+}) states. Trivalent chromium is an essential nutrient for glucose, lipid and protein metabolism in mammals, but it may be oxidized into hexavalent chromium ions which occur as highly soluble and highly toxic chromate anions (i.e. potentially carcinogenic) and it diffuse easily in cell membrane so, it has environmentally threats. Therefore the Cr^{6+} ions removal from water is significantly important for the human beings health. The contamination of water with Cr^{6+} ions exists from industrial processes as electroplating, pigment, metal cleaning, leather processing and mining. Many papers have been reported on the Cr^{6+} ions removal from wastewater [9-13]. Recycling of effluents becomes one of the most important trends to overcome the water deficiency problems and make it suitable for reuse [14-22]. The maximum permissible level reported by US regulations for Cr^{6+} ions discharges is 0.05 mg L^{-1} and the USEPA drinking water regulations limit the total chromium in drinking water to less than or equal to 0.1 mg L^{-1} [23,24]. Therefore, the affirmative treatment is required for detoxification of Cr^{6+} ions. The Cr^{6+} ions removal from water is obtained by a wide range of chemical and physical processes such as chemical precipitation, electrochemical reduction, cementation, reverse osmosis and elecrodialysis [25]. But these methods are restricted due to their disadvantages as high operational costs and problems of the residual sludge disposal that need further treatment. In contrast, the adsorption method is more efficiency and it has many advantages, it uses an inexpensive adsorbents, low operational costs and clean operation and economically feasible for Cr^{6+} ions removal [26].

Recently, different studies have been made to find inexpensive and effective adsorbents produced from cellulose as a natural polymer obtained from agricultural solid wastes. These types of adsorbents are particularly advantageous due to their properties as biocompatibility, biodegradability, good adsorption tendency, low-cost and highly available as starting materials and their appropriate chemical composition with high contents of carbohydrate polymers (e.g. cellulose and hemicelluloses) [27-33].

In this paper, we prepared 6-triethylenetetramine 6-deoxycellulose from rice husk cellulose and grafted with crotonaldehyde to improve cellulose capacity for adsorption of Cr^{6+} ions from wastewaters. The batch adsorption process was applied to evaluate the maximum adsorption capacity of proposed modified cellulose, and to study the isotherm and kinetic models. Adsorption parameters such as initial Cr^{6+} ions concentration, pH, contact time, and sorbent concentration were investigated.

2. MATERIALS AND METHODS

2.1 Materials

Sodium hydroxide scales, sodium hypochlorite, acetic acid, and hydrogen peroxide were purchased from El-Nasr Pharmacuitical Chemicals Co, Egypt. Dimethylacetamide, triethylamine, *p*-toluenesulfonyl chloride, ethanol, triethylenetetramine, dmethylsulfoxide, dimethylformamide, crotonaldehyde, acetonitrile, ferric chloride and $K_2Cr_2O_7$ were supplied by Merck and used without any further purification.

2.2 Isolation of rice husk cellulose

A 200 g of oven dried rice husk was taken in a 5 L round bottom flask and alkali treated with NaOH solution (4 L, 2%) in water bath at 70 °C for 2h. The reaction mixture was filtered and washed with tap water several times to eliminate black lacquer. The residual pulp was bleached firstly by sodium hypochlorite (4 L, 4% and 100 mL acetic acid) at 70 °C for 2h, then filtered and washed with tap water several times. Finally the residual pulp was again bleached by hydrogen peroxide H_2O_2 (4 L, 8%) at 70 °C for 2h then filtered and washed with distilled water. The produced white material was dried in an oven at 50 °C to give about 80 g cellulose which then pulverized to be ready for modification.

2.3 Chemical modification of rice husk cellulose

2.3.1 Preparation of tosylated rice husk cellulose

A 10 g of rice husk cellulose was heated in 240 mL of dimethylacetamide solvent at 130 °C, then cooled to 100 °C followed by addition of lithium chloride (20 g) with stirring until complete dissolution of cellulose (gives bright-yellow viscous solution) [8]. Cool the flask with solution in ice/water bath then add mixture of (50 mL dimethylacetamide/77 mL triethylamine base) to catalyze reaction with stirring at 8 °C. Then a solution of *p*-toluenesulfonyl chloride (52 g) in 110 mL dimethyl acetamide was added drop by drop through 1 h with stirring. The reaction was kept for 24 h in the refrigerator (4 °C). Add the reaction mixture to 2.5 L of cold water, then filtrated, washed with water, ethanol and dried at 50 °C for overnight.

2.3.2. Reaction of tosylated rice husk cellulose by triethylenetetramine

Triethylenetetramine (23 mL) and dimethylformamide (100 mL) were added to tosylated cellulose (10 g) in dimethylformamide (100 mL) and stirred at room temperature for 48 h. Then stirred at 60 °C for another 36 h, filtered, wash by ethanol and then dried overnight at 50 °C.

2.3.3. Grafting of Cell-TETA with crotonaldehyde

Cell-TETA (2.5 g) was reacted with 2.5 mL of crotonaldehyde in acetonitrile 50 mL in the presence of FeCl3 (300 mg) as catalyst at reflux for 24 h, cooled, filtered and dried overnight at 50 °C to give 3.2 g yield of Cell-TETA-crotonaldehyde (CTC).

2.4 Adsorption batch experiments

2.4.1 Preparation of Cr^{6+} solution

Initially, stock solution of Cr^{6+} ions (1000 mg L^{-1}) was prepared by dissolving the exact quantity of potassium dichromate in 1 L of double distilled water. Then, different Cr^{6+} ion solutions with adjustable concentrations were prepared by diluting the stock solution to the required initial concentrations. The required initial pH values were adjusted before mixing with (biomass) sorbent material using 0.1M HCl and 0.1M NaOH. Cr^{6+} ion concentration was measured using UV-visible spectrophotometric method based on the reaction of Cr^{6+} and diphenylcarbazide (Merck) which forms a red-violet colored complex [9-13, 34]. The absorbance of colored complex was measured in a double beam spectrophotometer (SPEKOL 1300-ANALYTIK JENA AG- Germany) at a wavelength, λmax 540 nm.

2.4.2 Effect of pH on metal adsorption

Studying of the effect of pH on the equilibrium uptake of Cr6+ ions was done by using 50 mg L^{-1} chromium concentration onto 2.0 g L^{-1} of CTC at different initial pH values (1.0–10.0). The samples were shaken at room temperature (25±2 °C) using agitation speed 200 rpm of orbital stirring shaker for the minimum contact time required to reach the equilibrium (120 min) and the amount of chromium adsorbed was determined.

2.4.3 Effect of CTC dose

The effect of CTC dose on the equilibrium uptake of chromium ions was performed by shaking of CTC (0.1, 0.15, 0.2, 0.25 and 0.30 g) with 100 mL of known chromium concentration (25, 50, 75, 100, and 150 mg L^{-1}), individually, meaning that, every Cr^{6+} concentration tested by shaking with all the above weights of (CTC) to the equilibrium uptake (120 min) and the amount of chromium adsorbed was determined [9-13]

2.4.4 Kinetics studies

Kinetic studies were completed by shaking of CTC (0.1, 0.15, 0.2, 0.25 and 0.30 g) individually with 100 mL of chromium solution (25, 50, 75, 100, and 150 mg L^{-1}) at room temperature (25±2 °C) at optimum solution pH (1.55). Samples of 50 µL were taken from each flask at definite time intervals and analyzed for residual chromium concentration in the solution [9-13].

2.4.5 Adsorption isotherm

Adsorption isotherm experiments were carried out in 250 mL conical flasks at 25 °C on a shaker for 120 min. The CTC (0.1, 0.15, 0.2, 0.25 and 0.30 g) were thoroughly mixed with 100 mL of chromium solutions. The isotherm studies were performed by varying the Cr^{6+} initial concentrations (25 to 150 mg L^{-1}) at constant pH value (1.55). After shaking the flasks for 120 min, the reaction mixtures were analyzed for the residual Cr^{6+} ions concentration. All the experiments are triplicated and only the mean values are reported with maximum deviation observed was less than ±5%.

3 RESULTS AND DISCUSSION

• [1]*Marine Pollution Department, Environmental Division, National Institute of Oceanography and Fisheries, Kayet Bey, Elanfoushy, Alexandria, Egypt*
• [2]*Chemistry Department, Faculty of Science, Damietta University, Damietta, Egypt*
**Corresponding author (Professor Dr. Ahmed El Nemr)*
e-mail: ahmedmoustafaelnemr@yahoo.com; ahmed.m.elnemr@gmail.com

The reaction of rice husk cellulose (**1**) with p-toluenesulfonylchloride in *N*,*N*-dimethylacetamide in the presence of triethylamine provided the cellulose tosylate **2** in good yield (90%). The tosylate **2** was reacted with excess of Triethylenetetramine (**3**) at 4 °C for overnight to give the proposed product 6-deoxy-6-triethylenetetramine cellulose (**4**) in good yield (85%). Compound 4 was then grafted with excess of crotonaldehyde in the presence of FeCl3 as catalyst [35-37] to give CTC in 88% yield of disubstituted product **5** (Fig. 1). The obtained products were identified using FTIR, EDX and SEM analyses.

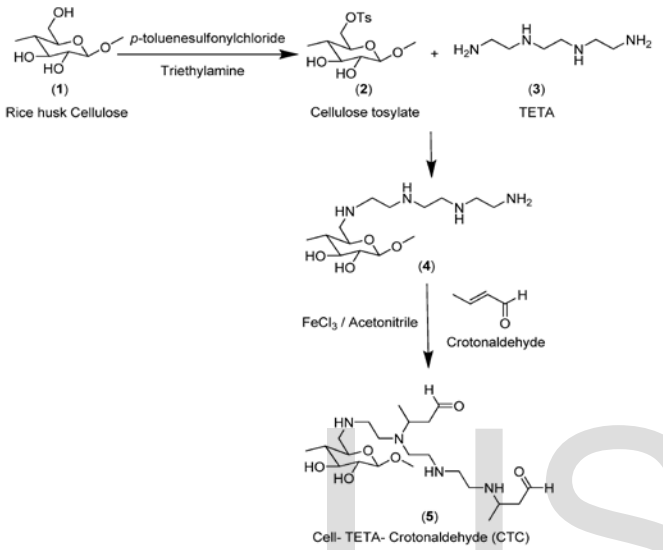

Fig. 1 Modification reaction of Cellulose to prepare Cell-TETA-crotonaldehyde.

3.1 Characterization of the chemically modified biosorbent

3.1.1 FTIR spectra of modified cellulose

The FTIR spectra of rice husk cellulose, the product of each step of modification, unloaded and loaded modified cellulose with Cr^{6+} were acquired with FTIR data were obtained using Bruker VERTEX 70 spectrometer in the range of 4000–400 cm^{-1} connected with Platinum ATR unit (Fig. 2 and 3). The infrared spectrum of rice husk cellulose and its modification showed band at 3450 cm^{-1} due to the elongation of the N–H and O–H bonds. Different functional groups were presented in the modified sample such as primary amines, secondary amines, carbonyl and alcohols. The band at 2852 cm^{-1} could be attributed to the C–H (CH_3, CH_2) bond elongation, this band is characteristic of materials with saturated carbons or SP^3. The band at 1630 cm^{-1} stretching frequency is characteristic of the C=O bond of an amide presented in CTC. The band at 1425 cm^{-1} is due to the C–O–H bond flexion; this band generally appears very close to the CH_2 bands. The broad band at 1021 cm^{-1} is due to the asymmetric stretching vibrations of C–O–C group which has been shifted to 1071 cm^{-1} after loading with Cr^{6+} ions. New band at 934 cm^{-1} could be attributed to Cr-O bond formation after Cr^{6+} loading. From the above observations it could be concluded that oxygen and nitrogen atoms play a major role in the adsorption of Cr^{6+} ions.

3.1.2 Scanning electron microscope (SEM) and Energy-dispersive X-ray spectroscopy (EDX) analyses

The field emission scanning electron microscopy (FE-SEM) was applied to study the surface morphology of CTC before and after loading with Cr^{6+} ions (Fig. 4). It could be observed that there is a distinct change in surface morphology after adsorption of Cr^{6+} since the pores in Fig 4a were completely filled with Cr^{6+} as shown in Fig. 4b. Fig. 5 shows the EDX plot of CTC samples before and after Cr^{6+} ions adsorption, respectively. Fig. 5b further confirmed the presence of chromium ions in the CTC samples.

The presence of chlorine in the CTC sample after Cr^{6+} ions adsorption may be attributed to the pH adjustment using HCl. The EDX analysis showed the presence of 11.29% of nitrogen that confirmed the chemical modification of cellulose with TETA (Table 1).

Table 1
EDX analysis data of CTC before and after Cr^{6+} ions adsorption process.

Elements	CTC before adsorption %	CTC after adsorption %
Carbon	54.39	54.30
Oxygen	30.26	21.30
Nitrogen	11.29	10.12
Sulfur	2.24	2.18
Chlorine	1.82	9.96
Chromium	0.00	2.14

3.2 Adsorption kinetics

The Cr^{6+} ions adsorption mechanism might be concluded as follows: (i) the negatively charged Cr^{6+} species (e.g. $HCrO_4^-$) migrated to the positively charged adsorbent surface sites (e.g. quaternary amine groups) mainly due to electrostatic driving forces. (ii) Cr^{6+} is converted to Cr^{3+} on the surface of the adsorbent through reduction by adjacent electron-donor groups at acidic conditions. The resulting Cr^{3+} can be then bound to anionic groups (e.g. hydroxyl and carboxyl groups) and form complexes with the chemical binding groups present in the adsorbent.

3.2.1 Effect of pH on Cr^{6+} uptake

The parameter, pH is the most important factor affecting the adsorption process on heavy metal as shown in the former studies [9-13]. The optimum pH for the effective adsorption of chromium ions by CTC was detected at different initial pH values (1.0–10.2). The difference of Cr^{6+} removal with initial pH is given in Fig. 6. Which shows that, the lowest uptake value was found at pH 8.2 and the highest uptake occurred at pH 1.0 and the uptake values decreased significantly with further increase in pH. At pH < 1, no more adsorption has mentioned than adsorption at pH 1. At optimum sorption pH, the

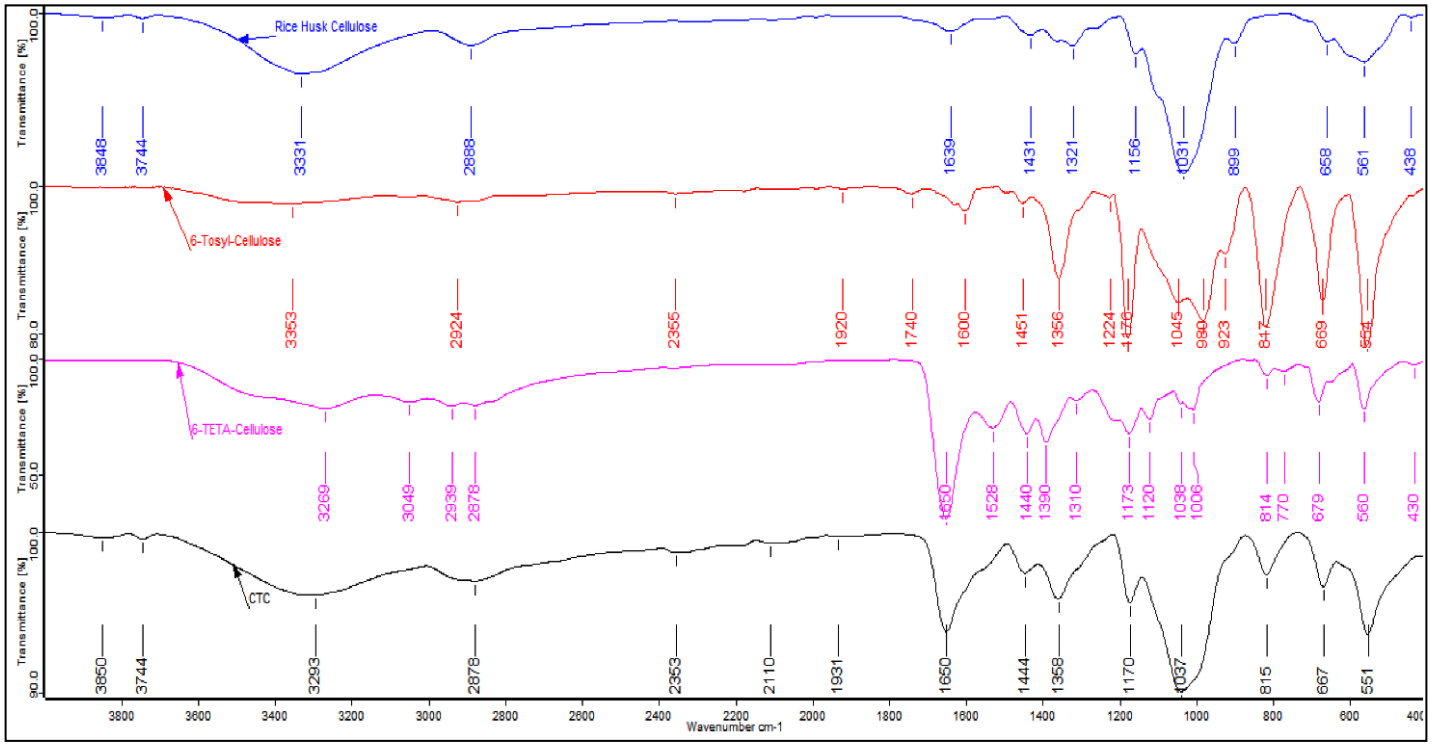

Fig. 2 FTIR spectral analysis of rice husk cellulose, 6-Tosyl cellulose, TETA-cellulose and Crotonaldehyde grafted TETA-cellulose.

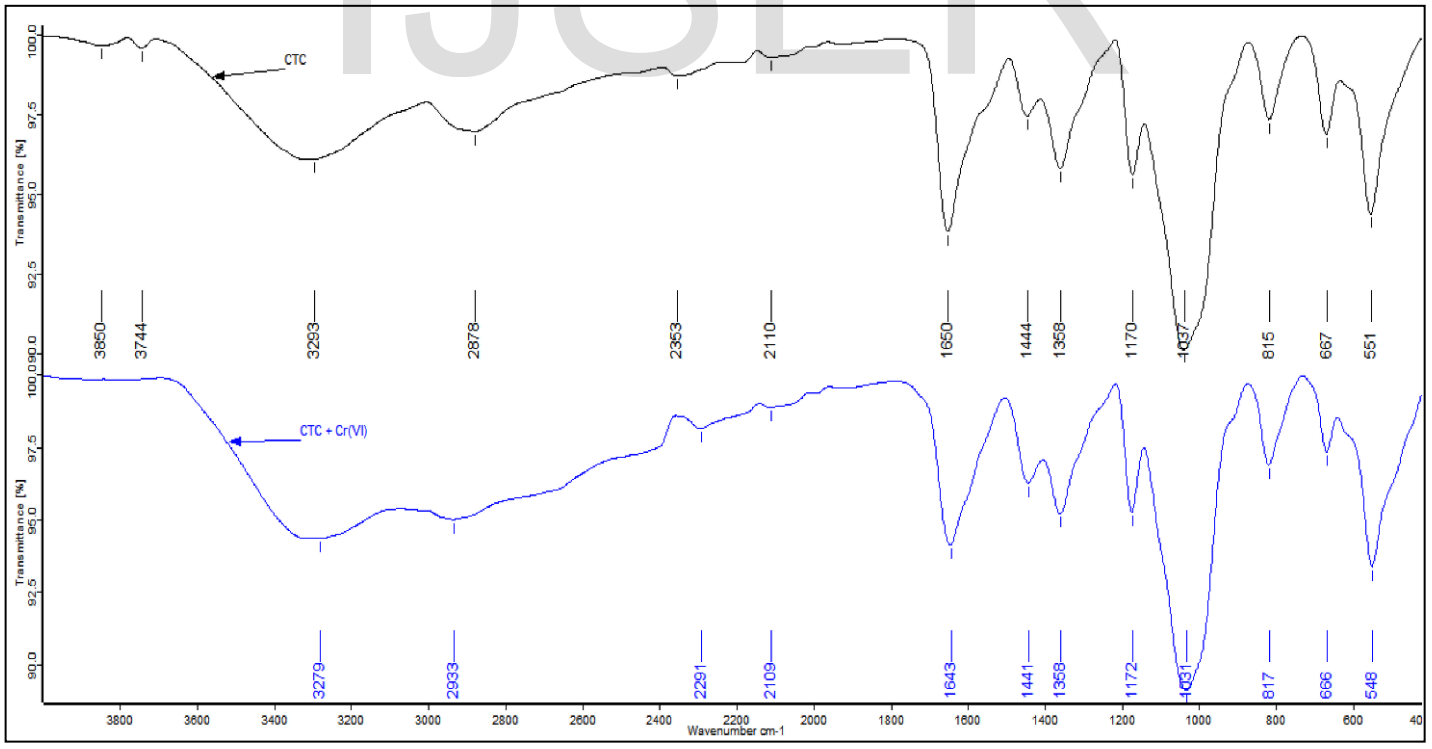

Fig. 3 FTIR spectral analysis of CTC before and after Cr^{6+} ions adsorption.

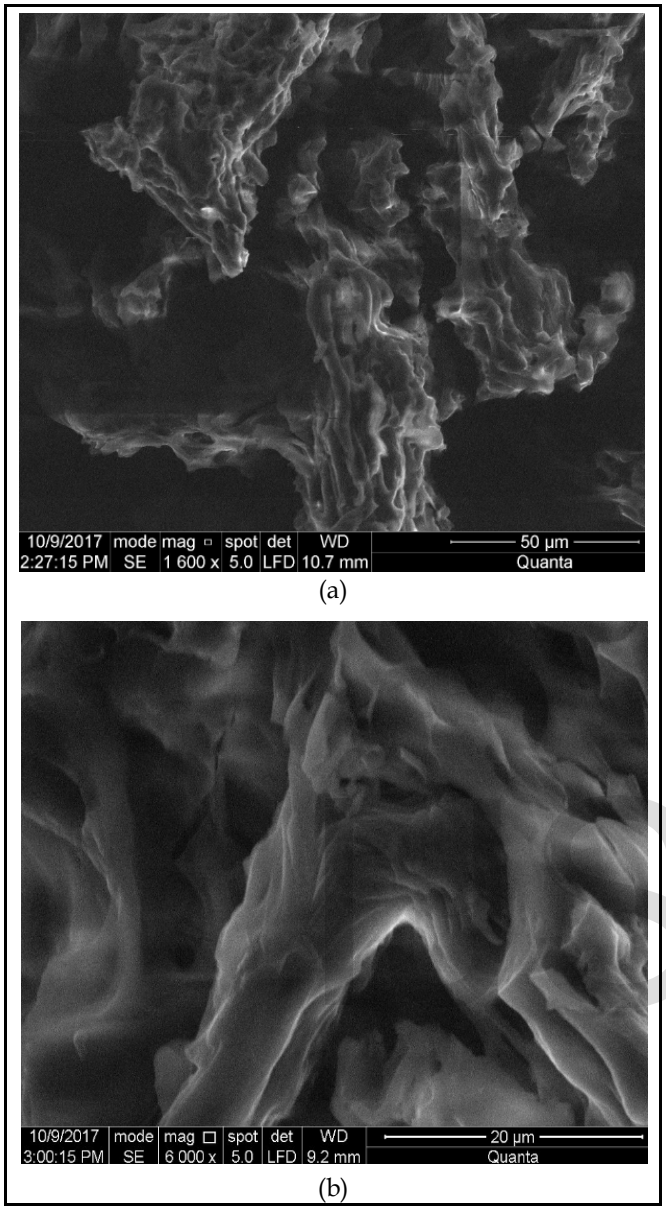

Fig. 4 (a) SEM of CTC before Cr^{6+} ions adsorption; (b) SEM of CTC after Cr^{6+} ions.

dominant species of Cr^{6+} ions in solution are $HCrO_4^-$, $Cr_2O_7^{2-}$, $Cr_4O_{13}^{2-}$ and $Cr_3O_{10}^{2-}$ which might be adsorbed mainly by electrostatically nature. At very low pH values, the surface of sorbent would also be surrounded by the hydronium ions which enhance the Cr^{6+} interaction with binding sites of CTC by greater attractive forces. As the pH increased, the overall surface charge on CTC became negative and adsorption of chromium decreased. Also, it has been known that in the case of high chromium concentration, the $Cr_2O_7^{2-}$ ions precipitate at higher pH values [9-15]. It should be mentioned that the form and valiancy of chromium ion are pH dependent; consequently the adsorption process depends on its form. Therefore, the percentage of removal and adsorption capacity are highly dependent on the solution pH value (Fig. 6).

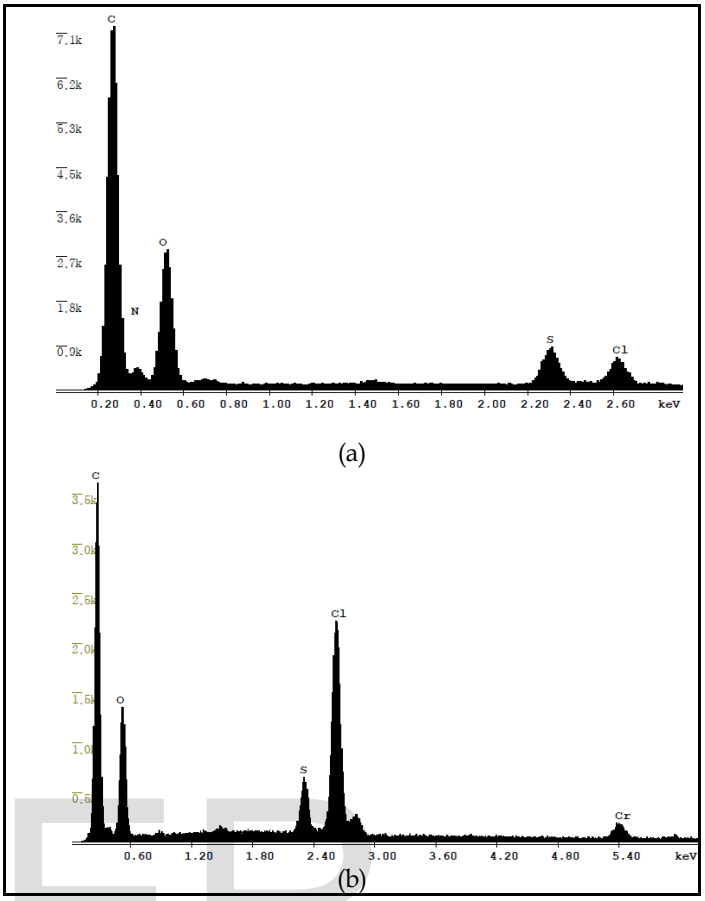

Fig. 5 (a) EDX plot of CTC before Cr^{6+} ions adsorption; (b) EDX plot of CTC after Cr^{6+} ions adsorption.

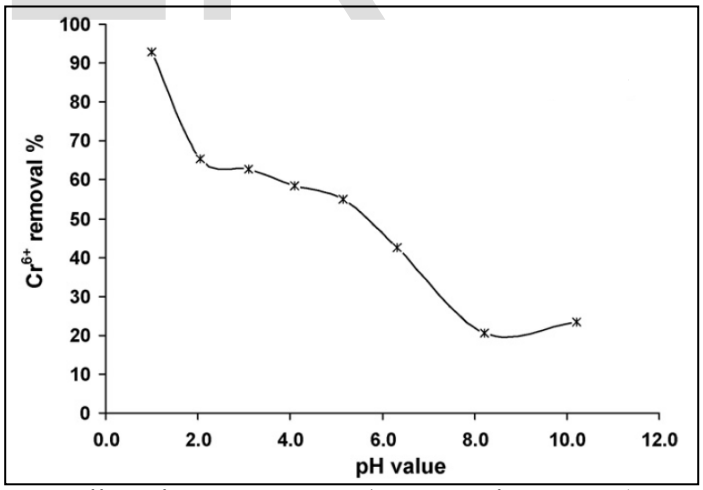

Fig. 6 Effect of system pH on adsorption of Cr^{6+} ions (75 mg L^{-1}) by CTC (6 g L^{-1}) at 25±2 °C.

3.2.2 Effect of contact time and initial Cr^{6+} ions concentration

The higher initial concentration of Cr^{6+} will increase the biosorption rate due to it offers an important role to overcome the mass transfer resistance of metal ion between the aqueous and solid phases. The results of percentage removal of Cr^{6+} at pH 1.55 with increasing of contact time using CTC are presented

in Fig. 7. The percentage of Cr^{6+} removal was increased with increasing time and CTC concentrations. Over 80% of Cr^{6+} was adsorbed in the time between 5 and 20 min, and thereafter the adsorption rate of Cr^{6+} onto CTC was found to be slow. That is probably occurred due to the electrostatic hindrance or repulsion between the adsorbed negatively charged Cr^{6+} on to the surface of CTC and the available anionic Cr^{6+} in solution as well as the slow pore diffusion of the Cr^{6+} ion into the bulk of CTC. The electrostatic interactions will be the major effect on the adsorption due to the presence of highly acidic solution (pH 1.55), which my control the adsorption via the attraction and repulsion between CTC surface and chromium ions.

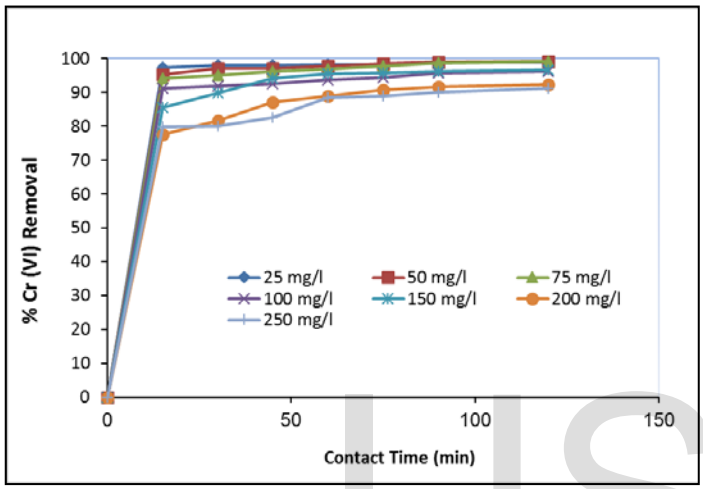

Fig. 7 Effect of contact time on the removal of different initial concentrations of chromium using CTC (4.0 g L^{-1}) at pH 1.55.

The relation between amounts of Cr^{6+} adsorbed at equilibrium (q_e) and its initial concentration using different doses of CTC are shown in Fig. 8. The equilibrium was found to be nearly 120 min when the maximum Cr^{6+} adsorption onto CTC was extended. In addition, the effect of initial Cr^{6+} concentration on the capacity of adsorption onto CTC is shown in Fig. 8, where percentage removal of Cr^{6+} determined at 120 min of contact time for seven different initial chromium concentrations is shown.

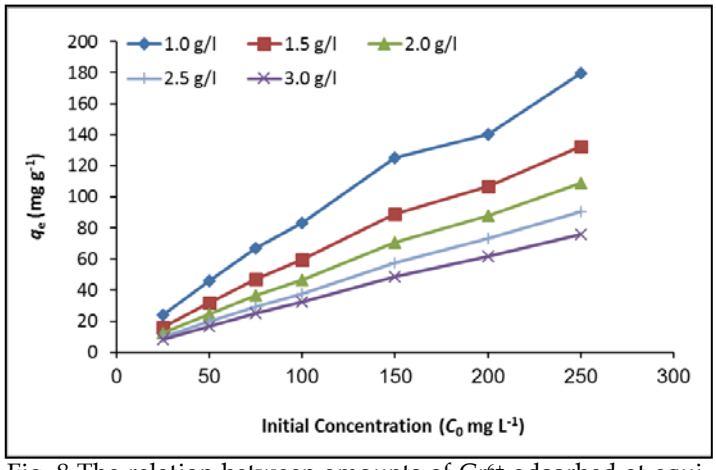

Fig. 8 The relation between amounts of Cr^{6+} adsorbed at equilibrium (q_e) and its initial concentration (C_0).

The removal percentage of Cr^{6+} ions decreased with the increasing of the initial chromium concentration and it can be concluded that the adsorption process may occur through electrostatic interactions.

3.2.3 Effect of adsorbent dose on metal adsorption

The effect of CTC dosage on the adsorption of Cr^{6+} from aqueous solutions was investigated using five different adsorbent concentrations and seven different initial chromium concentration. The amount of Cr^{6+} ions adsorbed is proportional to the available CTC specific area. Concentrations of CTC were varied from 1.0 to 3.0 g L^{-1} using initial chromium concentrations of 25 to 250 mg L^{-1} at pH 1.55. The equilibrium concentration (C_e) of Cr^{6+} ions decreases with increasing CTC concentration for a given initial Cr^{6+} ions concentration as shown in Fig. 9. The higher CTC doses provide the more sorbent surface area and increase the volume of pores which will be available for Cr^{6+} ions adsorption.

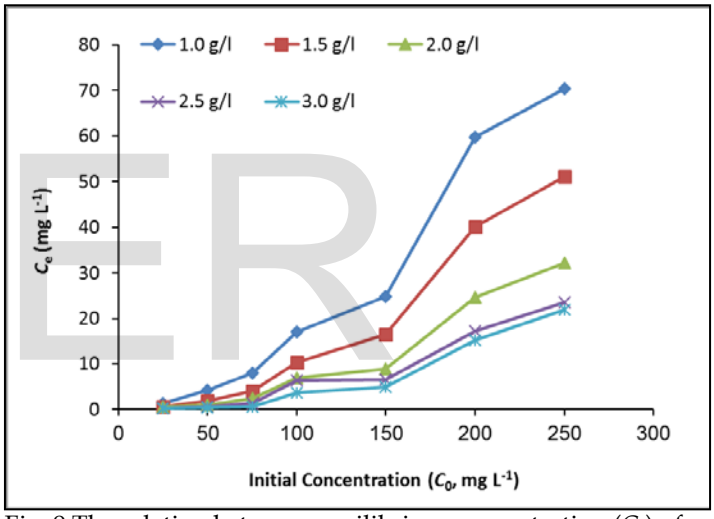

Fig. 9 The relation between equilibrium concentration (C_e) of Cr^{6+} ion and its initial concentration (C_0).

3.3. Isotherm data analysis

The adsorption of Cr^{6+} ions was studied at different initial chromium ion concentrations ranging from 25 to 250 mg L^{-1}, at optimum pH value (1.55) and at 200 rpm of the optimum agitation period. The isotherm data is important for column design purposes in treatment units. In addition, the isotherm data can be used to study how solute interacts with adsorbent and so is critical in optimizing the use of adsorbent. Langmuir and Freundlich isotherm models are the most widely accepted surface adsorption models for the single-solute systems. The data obtained were analyzed with the Langmuir, Freundlich, and Tempkin isotherm models. The best-fitting isotherm was tested by determination of the linear regression, and the parameters of the isotherms have been obtained from the intercept and slope of the linear plots of the different isotherm models.

3.3.1 Langmuir isotherm

At room temperature (25±2 °C), the adsorbed Cr^{6+} ions onto the CTC are in equilibrium with its ions in aqueous solution after 120 min contact time. The Langmuir model represents one of the first theoretical treatments of non-linear sorption and suggests that uptake occurs on a homogeneous surface by monolayer sorption without interaction between adsorbed molecules. In addition, the model assumes uniform energies of adsorption onto the surface and no transmigration of the adsorbate. Estimation of maximum adsorption capacity corresponding to complete monolayer coverage on the CTC was calculated using the Langmuir isotherm model since the saturated monolayer isotherm can be explained by the non-linear equation of Langmuir Eq. (1) [38].

$$\frac{C_e}{q_e} = \frac{1}{K_L Q_m} + \frac{1}{Q_m} \times C_e \qquad (1)$$

Where Ce is the equilibrium concentration (mg L^{-1}), q_e the amount of metal ion adsorbed (mg g^{-1}), Q_m a complete monolayer (mg g^{-1}) and K_L is an adsorption equilibrium constant (L mg^{-1}) that is related to the apparent energy of sorption. The results obtained from Langmuir model for the adsorption of Cr^{6+} onto CTC are shown in Fig. 10 and Table 1.

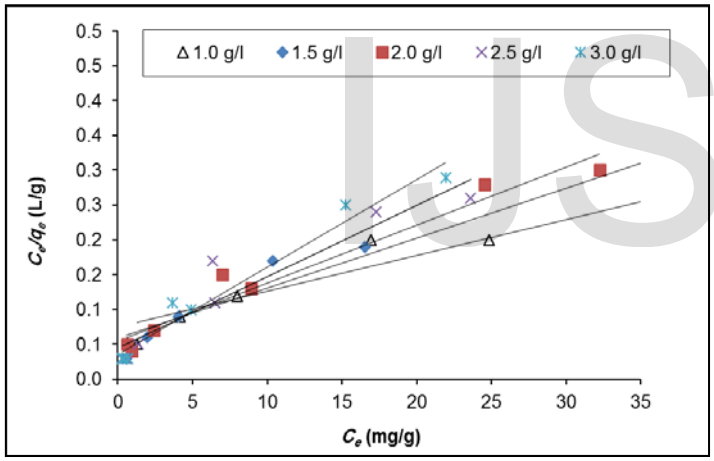

Fig 10 Langmuir isotherm of Cr^{6+} (25–250 mg L^{-1}) adsorbed onto CTC (1–3 g L^{-1}).

Table 1

Isotherm parameters obtained from the linear form of Langmuir, Freundlich and Tempkin models for the adsorption of Cr^{6+} onto CTC.

CTC / Isotherm	Isotherm parameter	1.0 g/ L	1.5 g/ L	2.0 g/ L	2.5 g/ L	3.0 g/L
Langmuir	Q_m (mg g^{-1})	196.1	138.9	120.5	98.0	80.0
	K_L (L mg^{-1})	0.07	0.12	0.16	0.23	0.35
	R^2	0.946	0.960	0.957	0.904	0.969
Freundlich	n	2.088	2.247	2.058	2.273	1.768
	K_F (mg g^{-1})	22.82	22.82	20.52	21.71	20.98
	R^2	0.978	0.986	0.944	0.944	0.914
Tempkin	A_t (L g^{-1})	0.99	2.17	2.43	5.06	6.70
	B_t (mg L^{-1})	36.81	24.59	22.67	16.25	13.79
	R^2	0.920	0.928	0.935	0.893	0.940

The results given in Table 1 show the possible applicability of the Langmuir to the adsorption of Cr^{6+} ions onto CTC proved by the low correlation coefficients. The maximum monolayer capacity, Q_m, obtained from Langmuir isotherm model for adsorption of Cr^{6+} ions onto CTC was 196.08 mg g^{-1}.

3.3.2 Freundlich isotherm

The Freundlich model was chosen for estimation of the adsorption intensity of the Cr^{6+} ions onto the CTC surface based on sorption heterogeneous energetic distribution of active sites accompanied by interactions between adsorbed molecules. It can be derived supposing a logarithmic decrease in the enthalpy of sorption with the increase in the fraction of occupied sites and is given by the following non-linear equation 2 [39]:

$$q_e = K_F C_e^{1/2} \qquad (2)$$

where K_F (mg g^{-1}) views for adsorption capacity and n for adsorption intensity of metal ions on the sorbent. Eq. (2) can be linearized in logarithmic form Eq. (3) and the Freundlich constants can be determined from the linear plot of log (q_e) against log (C_e).

$$\log q_e = \log(K_F) + \frac{1}{n} \log(C_e) \qquad (3)$$

The linear Freundlich isotherm plots for the adsorption of the Cr^{6+} ions onto CTC are presented in Fig. 11. Examination of the correlation coefficients reported in Table 1 shows that the Freundlich model is also has a possible applicability to CTC. The correlation coefficient obtained from CTC indicates that the experimental data fitted well to Freundlich model. The n values (1.168 - 2.273) are higher than 1.0, indicating that Cr^{6+} is favorably adsorbed by CTC at 25 °C. Moreover, the magnitude of KF ranged between (20.52 – 22.82), which indicates high adsorptive capacity and easy uptake of Cr^{6+} ions from aqueous solution by CTC.

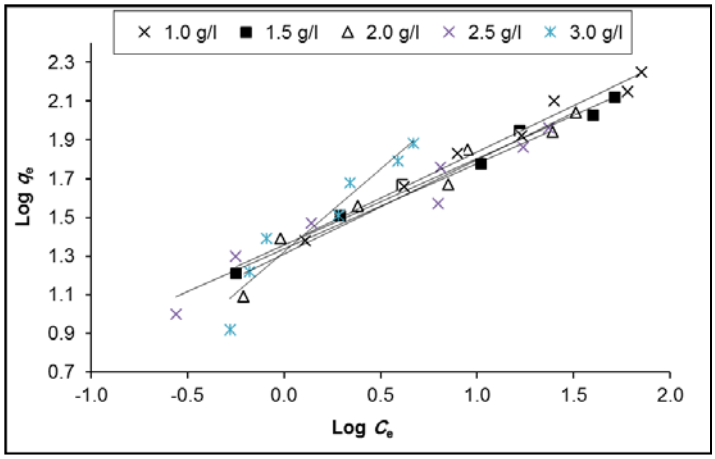

Fig. 11 Freundlich isotherm of Cr^{6+} ions (25–250 mg L^{-1}) adsorbed onto CTC (1–3 g L^{-1}).

3.3.3 Tempkin isotherm

Tempkin isotherm model measure the effects of indirect adsorbate–adsorbate interaction isotherms which describe that the heat of adsorption of all molecules on the adsorbent surface layer would decrease linearly with coverage due to adsorbate - adsorbate interactions. Therefore, the adsorption potentials of the adsorbent for adsorbates can be evaluated using Tempkin adsorption isotherm model, which accepts that the fall in the heat of sorption is linear rather than logarithmic, as implied in the Freundlich equation 2. The Tempkin isotherm has generally been applied in the following form Eq. (4) [40–42]:

$$q_e = (\frac{RT}{b}) \ln(A_T C_e) \quad (4)$$

The Tempkin isotherm Eq. (4) can be derived to the following equation (5):

$$q_e = B_T \ln(A_T) + B_T \ln(C_e) \quad (5)$$

where $B_T = (RT)/b$ and A_T (L g^{-1}) are the Tempkin constants and can be determined by a plot of qe against ln C_e (Fig. 12). Also, T is the absolute temperature in Kelvin and R is the universal gas constant, 8.314 J mol^{-1} K^{-1}. The constant b is related to the heat of adsorption [43,44]. The linear plots of the Tempkin isotherm Eq. (5) for the adsorption data are shown in Fig. 12. Examination of the data shows that the Tempkin isotherm is less applicable than Langmuir and Freundlich models to the adsorption of Cr^{6+} ions onto CTC due to the low correlation coefficients (Table 1).

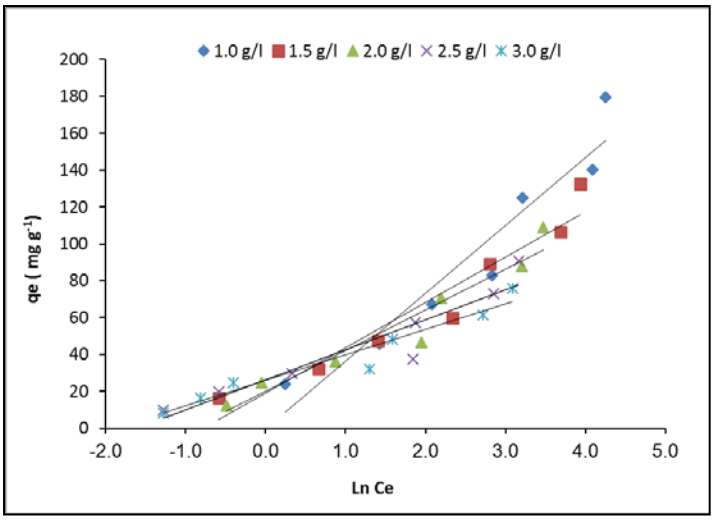

Fig. 12 Tempkin equilibrium isotherm model for the adsorption of Cr^{6+} ions (25–250 mg L^{-1}) onto CTC (1.0–3.0 g L^{-1}).

3.4 Kinetic studies

Batch experiments were shown to discover the rate of chromium adsorption by CTC at pH 1.55 with different chromium and CTC concentrations. The kinetic adsorption data can be treated to understand the dynamics of the adsorption reaction (i.e. the order of the rate constant). The kinetic of Cr^{6+} ions adsorption on CTC is essential for choosing optimum operating conditions for the full-scale batch process. Moreover, it is helpful to estimate the adsorption rate, gives important data for designing and modeling the processes. The chromium removal process from aqueous phase by CTC is studied by pseudo first-order [45], pseudo second order [46], intraparticle diffusion [47, 48] and Elovich [49–51] kinetic models. The conformity between experimental data and the model-predicted values was expressed by the correlation coefficients (R^2, values close or equal to 1).

3.4.1 Pseudo first-order kinetic model

The kinetic data were treated according to the Lagergren first-order model [45], which is the earliest one described the adsorption rate based on the adsorption capacity. It is generally stated in equation (6):

$$\frac{dq_t}{d_t} = k_1(q_e - q_t) \quad (6)$$

where qe and qt are the adsorption capacity (mg g^{-1}) at equilibrium and at time t, respectively, and k_1 is the rate constant of pseudo first-order adsorption (min^{-1}). Eq. (6) was integrated with the boundary conditions of time $t = 0$ to $t = t$ and $q_t = 0$ to $q_t = q_t$ and rearranged to the following linear equation (7):

$$\log(q_e - q_t) = \log(q_e) - \frac{k_1}{2.303} t \quad (7)$$

If the plotting of log ($q_e - q_t$) against (t) provides a linear relationship, the k_1 and predicted qe can be determined from the slope and intercept of the plot, respectively (Fig. 13). The difference in rate should be proportional to the first power of concentration for strict surface adsorption. However, the relationship between initial chromium concentration and rate of adsorption will not be linear when pore diffusion limits the adsorption process.

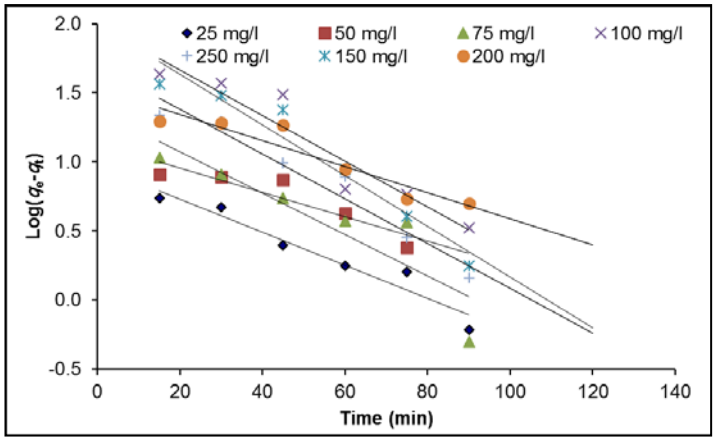

Fig. 13 Pseudo first-order kinetics for Cr^{6+} (25–250 mg L^{-1}) adsorption onto CTC (1.0 g L^{-1}) at pH 1.55 and temperature 25±2 °C.

It was observed from Fig. 13 that the Lagergren model does not fit the experimental data. On the other hand, the experimental qe values do not have a conformity with the calculated ones, obtained from the linear plots even when the correlation coefficient R^2 are relatively high (Table 2). This shows that the adsorption of Cr^{6+} ions onto CTC is not suitable to be described by a first-order reaction.

3.4.2 Pseudo second-order kinetic model

When adsorption kinetic data studied by the pseudo second-order model which given by Ho et al. [46] as shown in the following equation 8:

$$\frac{dq_t}{dt} = k_2(q_e - q_t)^2 \quad (8)$$

where k_2 (g mg^{-1} min^{-1}) is the second-order rate constant of adsorption. Integrating Eq. (8) for the boundary conditions q = 0 to $q = q_t$ at t = 0 to $t = t$ is linearized to obtain the following equation (9):

$$\frac{t}{q_t} = \frac{1}{k_2 q_e^2} + \frac{1}{q_e} \times t \quad (9)$$

The second-order rate constants were used to calculate the initial sorption rate (h), given by the following Eq. (10):

$$h = \frac{1}{k_2 q_e^2} \quad (10)$$

The second-order kinetics is applicable, if the plot of (t/q_t) against (t) shows a linear relationship. Values of k_2 and q_e were calculated from the intercept and slope of these plots (Fig. 14) which show good agreement between experimental and calculated q_e values at different initial Cr^{6+} ions and adsorbent CTC concentrations (Table 2) with correlation coefficients $R^2 \geq 0.999$. These high R^2 indicated that, the pseudo second-order kinetic model provided good correlation for the adsorption of Cr^{6+} ions onto CTC for all studied initial Cr^{6+} ions and adsorbent concentrations in dissimilarity to the pseudo first-order model. Moreover, values for the rate of initial adsorption, (h) mainly increased with the increase of the increase the initial Cr^{6+} ions concentration except for high CTC concentration (3 g L^{-1}) that gave mainly very close values of h, while the pseudo second-order rate constant (k_2) decreases with increase the initial Cr^{6+} ions concentration for all studied doses of CTC.

3.4.3 The intraparticle diffusion model

The adsorption process occurs in a multi-step involving the transport of solute molecules from the aqueous medium to the surface of the solid particles of adsorbate, followed by the diffusion of solute molecules into the interior of the pores, which is expected to be a slow process, and therefore, it can be considered as a rate-determining step. The intraparticle diffusion model had been explained by using the following equation (11) [47,48]:

$$q_t = K_{dif}\, t^{0.5} + C \quad (11)$$

where C is the intercept and K_{dif} (mg g^{-1} $min^{-0.5}$) is the intraparticle diffusion rate constant. The plot of (q_t) against ($t^{0.5}$) exist a multi-linearity correlation, which indicates that two or more steps occur during adsorption process (Fig. 15). The rate constant K_{dif} directly evaluated from the slope of the line and the intercept is C and is reported in Table 3. The values C provide information about the thickness of the boundary layer, since the resistance to the external mass transfer increases as the intercept increases. R^2 values given in Table 3 are ranged between 0.688 and 0.990, confirming that the rate-limiting step is actually the intra-particle diffusion process for some of the data analyzed when the R^2 values become close to 1.0. The linearity of the plots demonstrated that intra-particle diffusion played a significant role in the uptake of the chromium by

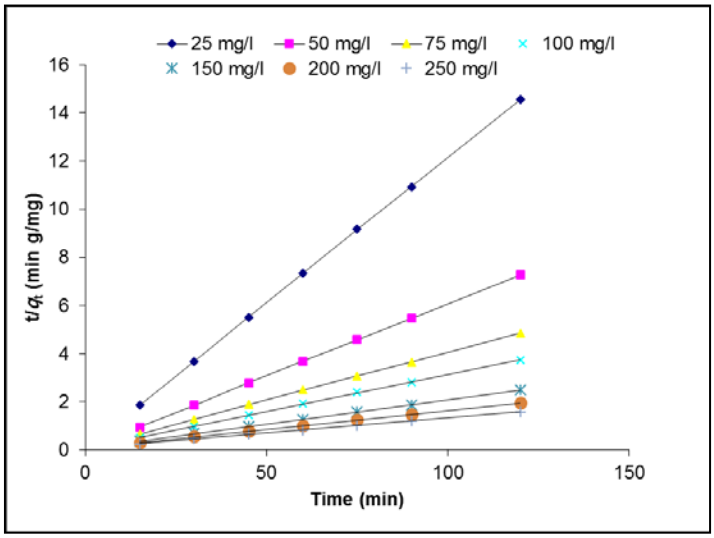

Fig. 14 Pseudo second-order kinetics for Cr^{6+} (25–250 mg L^{-1}) adsorption onto CTC (1.0 g L^{-1}) at pH 1.55 and temperature 25±2 °C.

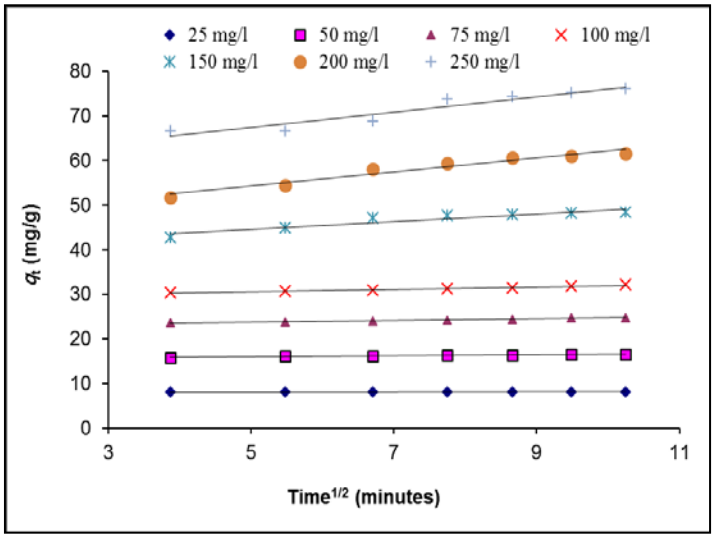

Fig. 15 The intraparticle diffusion kinetics for Cr^{6+} (25–250 mg L^{-1}) adsorption onto CTC (1.0 g L^{-1}) at pH 1.55 and temperature 25±2 °C.

Table 2

Comparison of the first- and second-order adsorption rate constants and calculated and experimental q_e values for different initial chromium and CTC weights.

Parameter			First-order kinetic model			Second-order kinetic model			
CTC conc (g L^{-1})	Cr^{6+} (mg L^{-1})	q_e (exp.) (mg g^{-1})	$k_1 \times 10^3$ (min^{-1})	q_e (calc.) (mg g^{-1})	R^2	$k_2 \times 10^3$ (g $mg^{-1}min^{-1}$)	q_e (calc.) (mg g^{-1})	h (mg $g^{-1}min^{-1}$)	R^2
1.0	25	23.72	27.636	9.369	0.938	4.992	25.06	3.14	0.998
	50	45.83	20.266	13.518	0.824	2.544	48.54	6.00	0.995
	75	67.00	34.545	23.518	0.793	2.817	69.44	13.59	0.999
	100	83.05	38.000	98.378	0.905	0.278	107.53	3.22	0.951
	150	125.17	42.145	99.793	0.942	0.624	136.99	11.71	0.995
	200	140.16	21.648	33.955	0.887	1.199	144.93	25.19	0.998
	250	179.55	37.309	50.478	0.948	1.422	185.19	48.78	1.000
1.5	25	16.30	40.533	6.907	0.970	10.025	17.12	2.94	0.999
	50	32.04	27.636	8.400	0.896	6.461	33.00	7.04	0.999
	75	47.30	37.539	18.950	0.942	3.561	49.51	8.73	0.999
	100	59.74	20.266	11.527	0.992	3.772	60.98	14.03	0.999
	150	88.96	37.769	39.473	0.943	1.894	108.70	22.37	0.998
	200	106.63	18.885	21.622	0.946	1.610	94.34	14.33	0.999
	250	132.55	12.897	17.730	0.729	2.123	133.33	37.74	0.998
2.0	25	12.19	61.490	2.148	0.864	70.853	12.35	10.70	1.000
	50	24.53	31.781	4.296	0.831	14.787	25.00	9.24	1.000
	75	36.31	33.624	9.623	0.924	6.656	37.45	9.34	1.000
	100	46.50	39.381	12.374	0.920	6.563	47.62	14.88	1.000
	150	70.53	41.684	30.052	0.935	3.720	72.46	19.53	1.000
	200	87.72	19.345	14.138	0.957	3.045	89.29	24.27	0.999
	250	108.89	15.660	15.011	0.857	2.689	109.89	32.47	0.999
2.5	25	9.89	21.418	0.314	0.991	163.354	9.92	16.08	1.000
	50	19.78	48.133	3.636	0.860	31.009	20.04	12.45	1.000
	75	29.44	12.897	1.378	0.739	26.693	29.59	23.36	1.000
	100	37.47	21.879	3.046	0.910	16.681	37.74	23.75	1.000
	150	57.40	32.242	7.700	0.956	8.831	58.14	29.85	1.000
	200	73.09	15.66o	10.240	0.967	3.797	74.07	20.83	0.999
	250	90.56	25.333	17.539	0.968	2.887	92.59	24.75	1.000
3.0	25	8.24	13.127	0.134	0.820	279.408	8.26	19.08	1.000
	50	16.52	35.236	1.218	0.937	64.385	16.64	17.83	1.000
	75	24.78	31.091	2.542	0.874	26.271	25.06	16.50	1.000
	100	32.11	24.872	3.097	0.868	17.217	32.47	18.15	1.000
	150	48.37	44.909	11.079	0.989	10.050	49.51	24.63	1.000
	200	61.59	39.842	20.941	0.988	3.673	63.69	14.90	1.000
	250	76.02	33.854	21.612	0.918	2.805	78.74	17.39	0.999

sorbent. The intra-particle diffusion rate constants, K_{dif}, were in the range of (0.02-7.69 mg g^{-1} $min^{-0.5}$). However, Fig. 15 shows low linearity for the adsorption of chromium by CTC which indicates that both of surface adsorption and intra-particle diffusion are involved in the rate-limiting step. However, still there is no sufficient indication about which of the two steps was the rate-limiting step. It has been reported [47,48] that if the intraparticle diffusion is the sole rate-limiting step, it is essential for the qt against ($t^{0.5}$) plots pass through the origin, which is not the case in this study. It may be concluded that surface adsorption and intraparticle diffusion were concurrently operating during the chromium-CTC interactions.

3.4.4 Elovich kinetic model

Elovich kinetic equation is another rate equation based on the adsorption capacity, which is generally expressed as follow in equation (12) [49-51]:

Table 3

The parameters obtained from intraparticle diffusion model and Elovich kinetics model using different initial Cr^{6+} concentrations and CTC doses.

Sorbent dose (g L^{-1})	Cr^{6+} conc. (mg L^{-1})	Intraparticle diffusion			Elovich		
		K_{dif} (mg g^{-1} $min^{-0.5}$)	C (mg g^{-1})	R^2	B (g mg^{-1})	α (mg g^{-1} min^{-1})	R^2
1	25	0.88	14.79	0.965	0.36	1.13E+02	0.957
	50	1.48	30.51	0.889	0.22	8.71E+02	0.812
	75	1.69	49.77	0.978	0.19	1.16E+04	0.966
	100	7.69	8.26	0.911	0.04	7.00E+00	0.887
	150	6.44	62.11	0.954	0.05	8.99E+01	0.930
	200	3.35	104.26	0.886	0.10	5.48E+04	0.827
	250	3.74	142.63	0.957	0.08	4.18E+05	0.940
1.5	25	0.54	4.14	0.891	0.58	2.24E+02	0.894
	50	0.80	23.96	0.953	0.39	5.50E+03	0.978
	75	1.40	33.50	0.969	0.23	1.73E+03	0.955
	100	1.22	46.72	0.990	0.26	1.32E+05	0.979
	150	3.40	56.67	0.925	0.09	3.58E+02	0.961
	200	2.25	82.11	0.962	0.14	1.51E+05	0.941
	250	2.43	106.07	0.815	0.12	7.88E+05	0.881
2	25	0.14	10.94	0.688	2.09	6.82E+108	0.778
	50	0.31	21.27	0.943	1.04	8.36E+108	0.879
	75	0.77	28.63	0.940	0.41	6.88E+04	0.919
	100	0.84	38.21	0.987	0.37	8.95E+05	0.977
	150	1.56	55.39	0.951	0.20	6.06E+04	0.971
	200	1.49	71.63	0.970	0.21	3.76E+06	0.952
	250	1.93	88.21	0.883	0.16	1.36E+06	0.932
2.5	25	6.22	21.52	0.948	9.35	$1.1E10^{37}$	0.981
	50	0.22	17.67	0.897	1.39	6.80E+109	0.927
	75	0.14	27.76	0.790	2.33	$1.19E10^{27}$	0.731
	100	0.35	33.88	0.885	0.88	$1.71E10^{12}$	0.929
	150	0.75	50.08	0.869	0.40	2.73E+108	0.925
	200	1.14	60.43	0.943	0.28	1.42E+07	0.928
	250	1.74	72.66	0.971	0.18	5.88E+05	0.955
3	25	0.02	8.04	0.895	16.61	$1.31E10^{56}$	0.884
	50	0.10	15.57	0.950	3.21	$3.06E10^{20}$	0.969
	75	0.20	22.75	0.990	1.62	$1.23E10^{15}$	0.956
	100	0.77	29.21	0.963	1.18	$1.82E10^{14}$	0.913
	150	0.87	40.21	0.882	1.16	$7.19E10^{17}$	0.931
	200	1.59	46.27	0.952	0.20	8.43E+03	0.970
	250	1.72	58.74	0.905	0.19	6.48E+04	0.862

$$\frac{dq_t}{dt} = \propto \exp(-\beta q_t) \quad (12)$$

Where α is the initial adsorption rate (mg g^{-1} min^{-1}) and β is desorption constant (g mg^{-1}) throughout any one trial of adsorption. It is shortened by supposing that $a\beta t >> t$ and by applying the limit conditions $q_t = 0$ at $t = 0$ and $q_t = q_t$ at $t = t$ in equation 12 to form equation 13. If Cr^{6+} adsorption by CTC undergoes the Elovich model, a plot of (qt) against ln(t) should give a linear correlation with a slope of $(1/\beta)$ and an intercept of $[(1/\beta)\times\ln(a\beta)]$ (Fig. 16).

$$q_t = \frac{1}{\beta}\ln(\propto \beta) + \frac{1}{\beta}\ln(t) \quad (13)$$

Thus, the constants can be obtained from the slope and the intercept of the straight line (Table 3). Relationship coefficients obtained by Elovich model were higher than that obtained from pseudo first-order model and comparable to that obtained from pseudo second-order model.

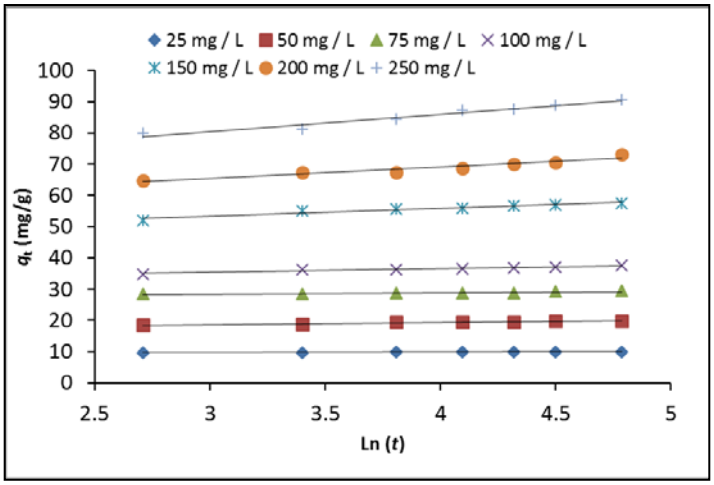

Fig. 16 Elovich kinetics for Cr^{6+} (25–250 mg L^{-1}) adsorption onto CTC (1.0 g L^{-1}) at pH 1.55 and temperature 25±2 °C.

The Cr^{6+} ions adsorption mechanism might be concluded as follows: (i) the negatively charged Cr^{6+} species (e.g. $HCrO_4^-$) migrated to the positively charged adsorbent surface sites (e.g. quaternary amine groups) mainly due to electrostatic driving forces. (ii) Cr^{6+} is converted to Cr^{3+} ions on the surface of the adsorbent through reduction by adjacent electron-donor groups at acidic conditions. The resulting Cr^{3+} can be then bound to anionic groups (e.g. hydroxyl and carboxyl groups) and form complexes with the chemical binding groups present in the adsorbent.

4 Conclusion

Chemical modification of the rice husk cellulose with triethylenetetramine then grafted using crotonaldehyde in the presence of $FeCl_3$ as catalyst provided a modified Cellulose-TETA-crotonaldehyde (CTC), which has been identified as an effective adsorbent to remove Cr^{6+} ions from various aqueous solutions. The adsorption process is pH dependent and the optimum pH was 1.55. Adsorption studies were modeled by followed Langmuir, Fruendlich and Tempkin isotherms. A high adsorption capacity of 196.08 mg g^{-1} was observed for Cr^{6+} ions. Furthermore, the isotherm equilibrium studies confirmed that the Fruendlich model and Tempkin models are the highest fitted models for the adsorption process of Cr^{6+} ions by CTC. The CTC showed high adsorption capacity under several initial chromium and sorbent dose concentrations. The Adsorbent–Adsorbate kinetic studies showed that the pseudo-second order kinetic was the applicable model. The adsorption process was found to be spontaneous and irreversible. The suggested modified sorbents are effective, environment friendly and can decrease the enormous amount of toxic chromium ions introduced into aquatic environment from effluent discharges as industrial electroplating industries urbanization. Applicability of the adsorbent derived from modified rice husk cellulose with triethylenetetramine then grafted by crotonaldehyde was successfully established for Cr^{6+} ions removal. Thus, CTC is found to be an efficient adsorbent for the removal of Cr^{6+} from aquatic environments.

Acknowledgment

The authors are thankful for the funding provided by STDF Project Number CB-4874 to carry out this work.

References

[1] O'Connell, D. W., Birkinshaw, C., O'Dwyer, T. F. "Heavy metal adsorbents prepared from the modification of cellulose: A review", Bioresource Technology 99 (2008) 6709–6724.
[2] Riaz, T., Ahmad, A., Saleemi, S., Adrees, M., Jamshed, F., Hai, A. M., Jamil, T. "Synthesis and characterization of polyurethane-cellulose acetate blend membrane for chromium (VI) removal", Carbohydrate Polymers 153 (2016) 582–591.
[3] Young, R.A. "cross-linked cellulose and cellulose derivatives", Absorbent Technology 2002.
[4] Roy, D., Semsarilar, M., Guthrie, J.T., Perrier, S. "Cellulose modification by polymer grafting: a review", Chemical Society Reviews, 38(7) (2009) 1825–2148.
[5] Alila, S., Boufi, S. "Removal of organic pollutants from water by modified cellulose fibers", Industrial Crops and Products, 30 (2009) 93–104.
[6] Hajeeth, T., Vijayalakshmi, K., Gomathi, T., Sudha, P.N. "Removal of Cu(II) and Ni(II) using cellulose extracted from sisal fiber and cellulose-g-acrylic acid copolymer", International Journal of Biological Macromolecules, 62 (2013) 59–65.
[7] Lui, C., Baumann, H. "New 6- butylamino-6-deoxycellulose and 6-deoxy-6-pyridiniumcellulosederivativeso of reaction", Carbohydrate research 340 (2005) 2229-2235.
[8] Hassaan, M. A., El Nemr, A., Madkour, F. F. "Environmental Assessment of Heavy Metal Pollution and Human Health Risk", American Journal of Water Science and Engineering, 2(3) (2016) 14-19.
[9] Abdelwahab, O., El Sikaily, A., Khaled, A., El Nemr, A. "Mass transfer processes of Chromium (VI) adsorption onto Guava seeds", Chemistry and Ecology, 23(1) (2007) 73-85.
[10] El Nemr, A., El Sikaily, A., Khaled, A., Abdelwahab, O. "Removal of toxic chromium (VI) from aqueous solution by activated carbon using *Casuarina Equisetifolia*", Chemistry and Ecology, 23(2) (2007) 119-129.
[11] El Nemr, A. "Pomegranate husk as an adsorbent in the removal of toxic chromium from wastewater", Chemistry and Ecology, 23(5) (2007) 409-425.
[12] El Nemr, A. "Potential of pomegranate husk carbon for Cr(VI) removal from wastewater: kinetic and isotherm studies", Journal of Hazardous materials, 161 (2009) 132-141.
[13] El Nemr, A., El Sikaily, A., Khaled, A., Abdelwahab, O. "Removal of toxic chromium from aqueous solution, wastewater and saline water by marine red alga *Pterocladia capillacea* and its activated carbon", Arabian Journal of Chemistry, 8 (2015) 105–117.
[14] Serag, E., El Nemr, A., Abdel Hamid, F. F., Fathy, S. A., El-Maghraby A. "A novel three dimensional Carbon Nanotube-polyethylene glycol - Polyvinyl alcohol Nanocomposite for Cu(II) removal from water", Egyptian Journal of Aquatic Biology and Fisheries, 22(2) (2018) 103-118.
[15] Hubbe, M. A., Hasan, S. H., Dusote, J. J. "Cellulosic Substrates for Removal of Pollutants from Aqueous Systems: A review. 1. Metals", Bioresources, (2011) 2161-2287.
[16] El Nemr, A., El-Sikaily, A., Khaled, A. "Modeling of adsorption isotherms of Methylene Blue onto rice husk activated carbon", Egyptian Journal of Aquatic Research, 36(3) (2010) 403-425.
[17] El-Sikaily, A., El Nemr, A., Khaled, A. "Copper sorption onto dried red alga *Pterocladia capillacea* and its activated carbon", Chemical Engineering Journal, 168 (2011) 707–714.
[18] Hassaan, M.A., El Nemr, A., Madkour, F.F. "Application of Ozonation and UV assisted Ozonation for Decolorization of Direct Yellow 50 in Sea water", The Pharmaceutical and Chemical Journal, 3(2) (2016) 131-138.
[19] Hassaan, M.A., El Nemr, A., Madkour, F.F. "Advanced Oxidation Processes of Mordant Violet 40 Dye in Freshwater and Seawater", Egyptian Journal of Aquatic Research, 43 (2017) 1–9.

[20] Hassaan, M.A., El Nemr, A., Madkour, F.F. "Testing the Advanced Oxidation Processes on the Degradation of Direct Blue 86 Dye in Wastewater", Egyptian Journal of Aquatic Research, 43 (2017) 11–19.
[21] Serag, E., El Nemr, A., El-Maghraby, A. "Synthesis of Highly Effective Novel Graphene Oxide-Polyethylene glycol-polyvinyl alcohol nanocomposite Hydrogel for Copper Removal", Journal of Water Environment and Nanotechnology, 2(4) (2017) 223-234
[22] El Nemr, A., Hassaan, M.A., Madkour, F.F. "Advanced oxidation process (AOP) for detoxification of acid red 17 dye solution and degradation mechanism", Environmental processes, 5 (2018) 95-113, DOI: 10.1007/s40710-018-0284-9
[23] EPA, USEPA Report no. EPA/570/9-76/003; Washington, DC, 1976.
[24] Patterson, R.R., Fendorf, S., Fendorf, M. "Reduction of hexavalent chromium by amorpous iron sulfide", Environ. Sci. Technol., 31 (1997) 2039–2044.
[25] El Nemr, A. (Editor), "Non-Conventional textile waste water treatment", Nova Science Publishers, Inc. Hauppauge New York. [Hard cover ISBN: 978-1-62100-079-2, e-book ISBN: 978-1-62100-228-4] (2012) 267 pages.
[26] Hokkanen, S., Repo, E., Sillapaa, M. "Removal of heavy metals from aqueous solutions by succinic anhydride modified mercerized nanocellulose", Chemical Engineering Journal, 223 (2013) 40-47
[27] Pillai, S. S., Deepa, B., Abraham, E., Girija, N., Geetha, P., Jacob, L., Koshy, M. "Biosorption of Cd(II) from aqueous solution using xanthated nano banana cellulose: Equilibrium and kinetic studies", Ecotoxicology and Environmental Safety, 98 (2013) 352–360.
[28] Haafiz, M. K. M., Hassan, A., Zakaria, Z., Inuwa, I.M. "Isolation and characterization of cellulose nano whiskers from oil palm biomass microcrystalline cellulose", Carbohydrate Polymers, 103 (2014) 119–125.
[29] Shin, H. K., Jeun, J. P., Kim, H. B., Kang, P. H. "Isolation of cellulose fibers from kenaf using electron beam", Radiation Physics and Chemistry, 81 (2012) 936–940.
[30] Mu, C., Jiang, M., Zhu, J., Zhao, M., Zhu, S., Zhou, Z. "Isolation of cellulose from steam-exploded rice straw with aniline catalyzing dimethyl formamide aqueous solution", Renewable Energy, 63 (2014) 324-329.
[31] Jiang, M., Zhao, M., Zhou, Z., Huang, T., Chen, X., Wang, Y. "Isolation of cellulose with ionic liquid from steam exploded rice straw, Industrial Crops and Products", 33 (2011) 734–738.
[32] Zhong, C., Wang, C., Huang, F., Jia, H., Wei, P. "Wheat straw cellulose dissolution and isolation by tetra-n-butylammonium hydroxide", Carbohydrate Polymers, 94 (2013) 38–45.
[33] Ratanakamnuan, U., Atong, D., Aht-Ong, D. "Cellulose esters from waste cotton fabric via conventional and microwave heating", Carbohydrate Polymers, 87 (2012) 84– 94.
[34] Snell, F.D., Snell, C.T. "Colorimetric Methods of Analysis, 3rd ed.", Inter Science, New York (1961).
[35] El Nemr, A., Khaled, A., Abdelwahab, O., El Sikaily A. "Adsorption of Direct Red 23 from Aqueous Solution Using Rice Husk Activated by Citric Acid" Environmental Science: An Indian Journal, 1(4-6) (2006) 86-98.
[36] Mousaad, A., Abdel Hamid, H., El Nemr, A., El Ashry, E.S.H. "Synthesis of 3-(Alditol-1-yl) triazolo[4', 3': 2, 3]-1, 2, 4-triazino[5, 6-b]indoles", Bulletin of the Chemical Society of Japan, 65(2) (1992) 546-552.
[37] El-Ashry, E.S.H., El Nemr, A. "Synthesis of mono-and di-hydroxylated prolines and 2-hydroxymethylpyrrolidines from non-carbohydrate precursors", Carbohydrate research, 338(22) (2003) 2265-2290.
[38] Langmuir, I. "The constitution and fundamental properties of solids and liquids", J. Am. Chem. Soc., 38 (1916) 2221–2295.
[39] Freundlich, U.H.M.F. "ber die adsorption in losungen", Zeitschrift fur Physikalische Chemie (Leipzig), 57A (1906) 385–470.
[40] Aharoni, C., Sparks, D.L. "Kinetics of soil chemical reactions-a theoretical treatment", in: Sparks, D.L.; Suarez (Eds.), D.L. Rate of Soil Chemical Processes, Soil Science Society of America, Madison, WI, (1991) 1–18.
[41] Aharoni, C., Ungarish, M. "Kinetics of activated chemisorption. Part 2", Theoretical models, J. Chem. Soc. Faraday Trans, 73 (1977) 456–464.
[42] Wang, X.S., Qin, Y. "Equilibrium sorption isotherms for of Cu2+ on rice bran", Process Biochem, 40 (2005) 677-680.
[43] Pearce, C.I., Lioyd, J.R., Guthrie, J.T. "the removal of color from textile wastewater using whole bacterial cells: a review", Dyes Pigments, 58 (2003) 179–196.
[44] Akkaya, G., Ozer, A. "Adsorption of acid red 274 (AR 274) on Dicranella varia: determination of equilibrium and kinetic model parameters", Process Biochem, 40 (11) (2005) 3559–3568.
[45] Lagergren, S. "Zur theorie der sogenannten adsorption geloster stoffe", Kungliga Svenska Vetenskapsakademiens, Handlingar, 24 (1898) 1–39.
[46] Ho, Y.S., McKay, G., Wase, D.A.J., Foster, C.F. "Study of the sorption of divalent metal ions on to peat", Adsorpt. Sci. Technol., 18 (2000) 639–650.
[47] Weber, W.J., Morris, J.C. "Kinetics of adsorption on carbon from solution", J. Sanit. Eng. Div. Am. Soc. Civ. Eng., 89 (1963) 31–60.
[48] Srinivasan, K., Balasubramanian, N., Ramakrishan, T.V. "Studies on chromium removal by rice husk carbon", Ind. J. Environ. Health, 30 (1988) 376–387.
[49] Zeldowitsch, J. "Uber den mechanismus der katalytischen oxidation von CO an MnO2", Acta Physicochim. URSS, 1 (1934) 364–449.
[50] Chien, S.H., Clayton, W.R. "Application of Elovich equation to the kinetics of phosphate release and sorption on soils", Soil Sci. Soc. Am. J. , 44 (1980) 265–268.
[51] Sparks, D.L. "Kinetics of reaction in Pure and Mixed Systems in Soil Physical Chemistry", CRC Press, Boca Raton, (1986).